Food & Function

Accepted Manuscript

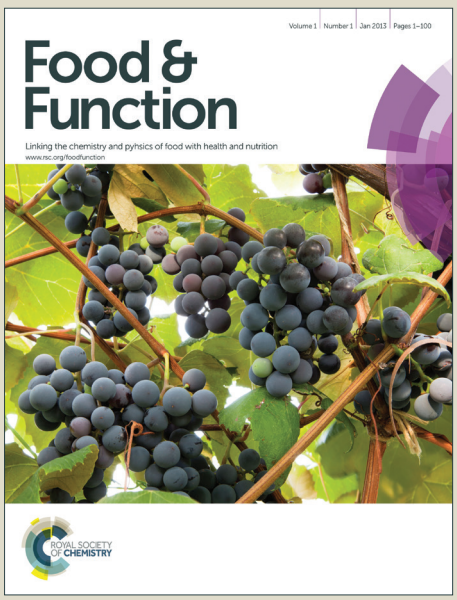

This is an *Accepted Manuscript*, which has been through the Royal Society of Chemistry peer review process and has been accepted for publication.

Accepted Manuscripts are published online shortly after acceptance, before technical editing, formatting and proof reading. Using this free service, authors can make their results available to the community, in citable form, before we publish the edited article. We will replace this *Accepted Manuscript* with the edited and formatted *Advance Article* as soon as it is available.

You can find more information about *Accepted Manuscripts* in the Information for Authors.

Please note that technical editing may introduce minor changes to the text and/or graphics, which may alter content. The journal's standard Terms & Conditions and the Ethical guidelines still apply. In no event shall the Royal Society of Chemistry be held responsible for any errors or omissions in this *Accepted Manuscript* or any consequences arising from the use of any information it contains.

ROYAL SOCIETY OF CHEMISTRY

www.rsc.org/foodfunction

Food & Function

RSCPublishing

ARTICLE

Cartilage polysaccharide induces apoptosis in K562 cells through a reactive oxygen species-mediated caspase pathway

Wei Song,*[a] Panpan Hu,[a] Yujuan Shan,[a] Ming Du,[a] Anjun Liu*[b] and Ran Ye[c]

Cite this: DOI: 10.1039/x0xx00000x

Received 00th January 2012,
Accepted 00th January 2012

DOI: 10.1039/x0xx00000x

www.rsc.org/

In this study, a polysaccharide (PS) was successfully extracted from porcine cartilage and its effect on chronic myeloid leukemia was examined using human K562 cells. The results of cell proliferation assays indicated that the PS inhibited cancer cell growth at different concentrations. Morphological and biochemical changes characteristic of apoptosis were observed and confirmed with PI staining and TUNEL assay. The nuclear DNA, RNA and proteins of the cancer cells were irreversibly destroyed by reactive oxygen species (ROS) subjected to PS treatment, additionally, the ROS effected on the cells directly. The apoptotic signals altered the permeability of the mitochondrial outer membrane, thereby resulted in the release of apoptotic factors into the cytoplasm that induced apoptosis. As caspase-3/7, 8 and 9 were expressed, it was speculated that both intrinsic and extrinsic pathways were involved in the PS-induced apoptosis.

Introduction

In recent years, polysaccharides have received increasing attention due to their antitumor and antioxidant activities, immune responses and other biological activities.[1, 2] Most of the related reports concern the functions of polysaccharides obtained from plant sources and microorganisms that include Lingzhi mushroom and lactic acid bacteria.[3,4] Recently, numerous studies indicated that polysaccharides with animal origins mainly consisting of glycogen, chitosan, heparin, chondroitin sulfate, hyaluronic acid, etc.[5, 6], possessed multiple anticancer, anti-inflammatory, and antiviral properties; can regulate blood glucose and blood lipids; and enhance immunity with almost no toxic effects.[7-10]

Our previous study revealed that porcine polysaccharide (PS) extracted from porcine cartilage by our laboratory induced apoptosis in K562 and MCF-7 cells through the MAPK pathway and the caspase-8-mediated Fas pathway.[10, 11] Caspase is considered to play a crucial role in the initiation and execution of apoptosis.[12-14] Furthermore, it is demonstrated that MAPK pathways are responsible for reactive oxygen species (ROS)-mediated apoptosis.[15-17] Thus, the effects of caspase and ROS on PS-induced K562 apoptosis urgently need to be identified.

It has recently been found malignant cells produce certain amounts of ROS, including superoxide anions (O_2-·) and hydrogen peroxide (H_2O_2),[11] via autocrine mechanism. However, ROS can be eliminated by intracellular antioxidant enzymes superoxide dismutase (SOD), catalase (CAT) and glutathione (GSH). Cell survival depends on the balance of intracellular ROS and antioxidative metabolism, and this balance reflects the in vivo redox status.[18, 19] Mitochondria are the major site of the production of intracellular ROS that are the products of the normal cellular metabolism; however the mitochondria can also be involved in apoptosis under certain conductive conditions.[20, 21] In particular, ROS could induce oxidative stress and can destroy DNA, RNA and protein leading to cell apoptosis or death.[22, 23] Moreover, ROS participates in apoptotic processes as signaling molecules.[24] External stimulation causes the changes of mitochondrial membrane potentials and mitochondrial membrane permeabilities, [21] and cytochrome c is released to stimulate the accumulation of ROS, which aggravates the intracellular oxidation state.[25] Afterwards, this process stimulates a series of events that this process induces mitochondria-mediated apoptotic pathways.[26]

Tumor cell apoptosis is mainly mediated through the exogenous death receptor pathway and the endogenous mitochondrial pathway.[27] The tumor necrosis factor superfamily, which includes Fas, DR4/5, TNFR1, and Fas/FasL, is involved in death receptor-induced apoptosis. These factors combine to initiate the apoptotic signaling pathway, the subsequent activation of caspase-8, and, ultimately, the induction of apoptosis.[28-30] The endogenous apoptotic pathway is mediated by mitochondria.[27] Following stimulation from an external factor, the mitochondrial membrane potential ($\Delta\psi m$) of the cell is altered to induce and enhancement of mitochondrial membrane permeability and also the release of cytochrome c into the cytoplasm, which activates caspase-9, which in turn activates the death signal caspase-3. The endogenous mitochondrial and exogenous death receptor pathways activate caspase-3 and apoptotic effector molecules to simultaneously induce apoptosis.[27, 31] In this study, the anti-tumor and cellular redox state effects of a polysaccharide extracted from porcine

cartilage were studied in K562 cells. We hypothesized that the apoptotic effect of the PS in K562 cells is mediated by the ROS-mediated caspase pathway.

Materials and Methods

2.1 Cell lines and materials

K562 cells were presented by the immune laboratory of Tianjin Medical University and were passaged in RPMI-1640 (Gibco, USA) containing 10% heat-inactivated fetal bovine serum (FBS) (Sigma, USA), 100 U/ml penicillin G, 100 μg/ml streptomycin, and 2 mmol/l glutamine. MTT, cytochrome C, RnaseA and PI were purchased from Sigma–Aldrich Chemical (St. Louis, MO, USA). SOD test kits were obtained from Nanjing Jiancheng Bioengineering Institute (Nanjing China). TritonX-100, Coomassie brilliant blue G250 and DMSO were purchased from the Beijing Lianxing Biotechnology Company. All other chemicals were of analytical grade and obtained in China.

2.2 Preparation of the short-chain polysaccharide from the cartilage

The extraction and purification of the polysaccharide from the porcine cartilage are described in our previous study.[10] Generally, specific amounts of porcine cartilage were treated with sodium carbonate for 3 h and then heated at 70° and mixed for 30 min. Degradation with papain was performed, and the substance was purified with a DEAE-Sephadex A-25 column and degraded with hydroxyl radicals to produce a short-chain polysaccharide (PS). The PS was then precipitated by ethanol. After lyophilization, the PS was dissolved in cell culture medium for further study.

2.3 HPLC analysis

HPLC analysis of the PS from the porcine cartilage was performed on a SSI PC-2000 HPLC system equipped a diode-array UV-visible detector (SSI, model 500). The analyses were performed on a Zorbax SB C18 column (250 mm ×4.6 mm, i.d. 5μm). The UV detector was set to a wavelength of 195 nm. The eluant contained 10.0% acetonitrile and 0.08% orthophosphoric acid, and 0.12% octane sodium p-aminobenzenesulfonate was used in the HPLC runs at a flow rate of 0.6 ml/min. The results are the averages of triplicate experiments using chondroitin sulfate as the standard.

2.4 Cell proliferation assay

The cells were transferred to 96-well plates containing RPMI-1640 medium supplemented with 0.5% FBS. The optimal cell number/well for the cells was found to be 2×10^4 cells/well based on titration assays. The cells were allowed to settle overnight and were incubated with various concentration of PS (25μg/ml, 100μg/ml, 200μg/ml, 400μg/ml and 800μg/ml) for an additional 3 days at 37° in a humidified 5% CO_2 incubator. After each day of incubation, MTT solution (0.5 mg/ml in phosphate-buffered saline (PBS)) was added for 4 h of incubation at 37°. The precipitated formazan was dissolved in 150 μl DMSO, and the plates were read at 570 nm using a microplate reader (Model 680, Bio-Rad, Hercules, CA, USA). All experiments performed in triplicate.
The percent growth inhibition was defined as follows: [(absorbance of the control (cells treated without PS))–(absorbance of the treated cells)] / absorbance of the control x 100.

2.5 PI Staining

The morphological changes of the cells that were treated with PS were evaluated with PI staining. Briefly, the K562 cells were treated with 100 μg/ml PS for 24 h. The cells were then harvested at a concentration of 1×10^6 cells/ ml, washed in ice-cold PBS twice, and then suspended in 160 μl PBS. The cells were stained with 50 μg/ml PI for 15 min at room temperature in the dark. After centrifugation, the pastes were dispersed in PBS and cytospun on slides. The specimens were examined and photographed under a fluorescence microscope (Olympus, C5060-ADU, Tokyo, Japan).

2.6 TUNEL assay

The extent of the in vitro induction of apoptosis due to the cartilage polysaccharide treatment was determined by the TUNEL Cell Biol Toxicol assay with an in situ apoptosis detection kit (Promega, Madison, WI, USA). Briefly, K562 cells were cultured with different concentrations of PS for 24h. After harvested and washed with PBS, cell suspension was pipetted onto the slides at a concentration of 1×10^6 cells/ml. The rTdT incubation buffer was added to the cells and the slides were incubated at 37° for 60min inside the humidified chamber. The reactions were terminated by immersing the slides in 2×SSC in a Coplin jar for 15 min at room temperature. The slides were then washed with fresh PBS for 5 min. The specimens were examined and photographed under a fluorescence microscope (Olympus, C5060-ADU, Tokyo, Japan).

2.7 Detection of superoxide anions

The K562 cells were adjusted to 1×10^5 cells/ml in no-phenol red medium and seeded into 6-well plates at 5 ml per well. Cytochrome C was added to the continuing cultures of the experimental groups at a final concentration of 12.5 μmol/l at 12 h, 24 h and 48 h with 100 μg/ml of PS. The plates were read at 550 nm, and wells without PS were used as controls. Superoxide anion levels are expressed as nmol/10^6 cells according to method of Szücs, S. et al.[32]

2.8 Detection of superoxide dismutase (SOD) and catalase (CAT) activities

Cells in the log phase were adjusted to 1×10^5 cells/ml and seeded into 6-well plates at 5 ml per well. After incubation with 100 mg/l PS for 12 h, 24 h and 48 h, approximately 10^6 cells were collected to and centrifuged for 7.5 min. The cells were washed twice with cold PBS (pH 7.4), and the cell pellet was lysed via the addition of Triton X-100 at 4° for 30 min. The supernatant was obtained following centrifugation at 14000 rpm for 10 min. The xanthine oxidase method was used to detect the SOD activity following the manufacturer's instructions. To detect the CAT activity, H_2O_2 was used as a substrate, and the consumption was quantified spectrophotometrically at 240 nm using a plate reader.

2.9 Analysis of the caspase activities

The activities of caspases 3/7, -8 and -9 were detected with a Caspase-Glo 3/7, 8, and 9 assay system (Promega). After preincubation with or without 100μg/ml PS for 4, 8, 12, 24, or

48 h, the K562 cells (2×10^4 cells/well) in the 96-well plates were centrifuged at 200 g for 10 min. Subsequently, the supernatant was removed, and 100 μl of Caspase-Glo 3/7, 8, 9 reagent was added to each well. The context of the wells were gently mixed using a plate shaker at 300 rpm for 30 s and were then incubated at room temperature for 1 h. The luminescence of each sample was measured in a plate-reading luminometer.
The fold increases in enzyme activities were calculated as (assay value - blank value) / (negative control value - blank value).

2.10 Statistics

All of the presented data and results were conducted using at least three independent experiments. The data are expressed as the means ± the SDs. The differences between groups were assessed using SPSS software. The results were considered to be statistically significant when the p value was < 0.01.

Results and discussion

3.1 Extraction of PS

The yield of PS was 23.7% based on the extraction method described in the section 2.2 and the dry mass of the porcine cartilage (data not shown). PS at a concentration of 0.4 mg/ml was used to determine the purity of the samples with the HPLC system as described in section 2.3. Compared to the standard, only a small peak appeared next to the main peak as shown in Fig. 1. The PS from the porcine cartilage exhibited 95% chondroitin sulfate purity according to calculations based on the internal standard method. Moreover, in our previous study, the sample was run in parallel on a polyacrylamide gel. The protein staining by Coomassie blue R-250 also demonstrated that the sample was pure. Alcian blue staining revealed that the average molecular weight of the PS was approximately 30 kDa.[10]

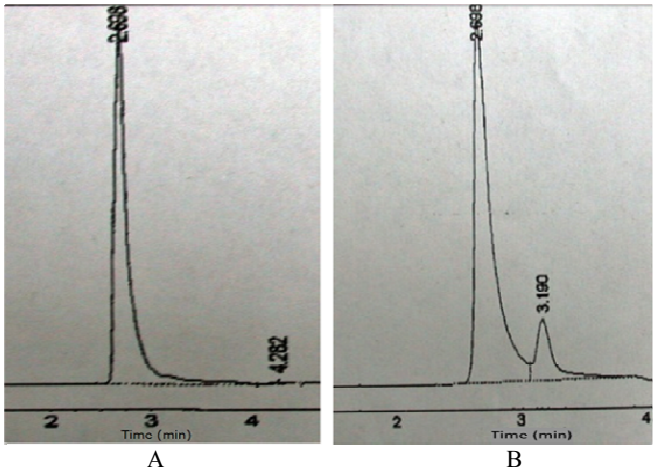

A B

Fig.1 HPLC profile of the polysaccharide from porcine cartilage. Molecular weight determination was performed on a Zorbax SB C18 column (250 mm ×4.6 mm, i.d. 5μm) with 10.0% acetonitrile, 0.08% orthophosphoric acid and 0.12% octane sodium p-aminobenzenesulfonate at 0.6 ml/min. A: chondroitin sulfate Standard; B: PS sample

3.2 Inhibitory effect of PS on K562 cell ProliferationK562 cell proliferation assays were performed to determine the bioactivity of the polysaccharide extracted from the porcine cartilage. The difference between the control and PS-treated cultures was statistically significant ($p<0.05$). PS dose-dependently inhibited cell proliferation after 48 h and 72 h treatments as shown in Fig. 2. The inhibitory effect of 800 μg/ml short-chain PS on K562 cell proliferation was similar to that of 100 μg/ml PS. Therefore, 100 μg/ml PS was used for the subsequent experiments.

3.3 Examination of the morphologies following the PS treatments

The morphological changes in the cells that were treated with PS were evaluated with PI staining. First, the cells were treated with or without 100 μg/ml PS for 24 h. The cells were then stained with PI via conventional methods and photographed under a fluorescence microscope. Among the control cells, the nucleus occupied nearly the entire cell (Fig. 3A, 3B). The presence of morphological indicators of apoptosis, such as nuclear shrinkage, was observed following PS treatment in the PI-stained sections (Fig. 3C, 3D). The numbers of apoptotic cells increased remarkably, and the nuclei had nearly completely disappeared comparing with the control. Thus, the PI staining indicated that apoptosis occurred following PS treatment in K562 cells.

3.4 Induction of apoptosis by PS

As illustrated in Fig. 4A-E, TUNEL staining was conducted to determine whether, in addition to its effects on cell proliferation, PS also regulates cell survival. As demonstrated in Fig. 4F, the apoptotic rate increased in a dose-dependent from 4.87%±1.21% in the control group to 35.67%±4.04% in the experimental group that was treated with 50 μg/ml PS and to approximately 50% in the groups that were treated with 100–400 μg/ml PS. Combing with the results described in Fig. 2, these findings indicate that the rate of apoptosis was positively correlated with the rate of the proliferation of inhibition under 24 h and with increasing concentrations. These data suggest that the PS prevented cell survival and induced apoptosis in the human K562 cells.

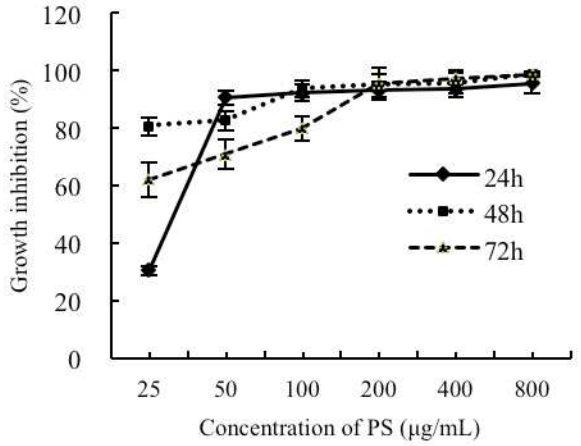

Fig.2 Cell proliferation of K562 cells treated by PS. Under the effect of various concentrations of PS: 25 μg/ml, 50 μg/ml, 100 μg/ml, 200 μg/ml, 400 μg/ ml, and 800 μg/ml, K562 cells were incubated for 24h, 48h, 72h, respectively. Results represented the mean ± SD of triplicate cultures and were expressed as percentage of control. Error bars represented the standard deviation.

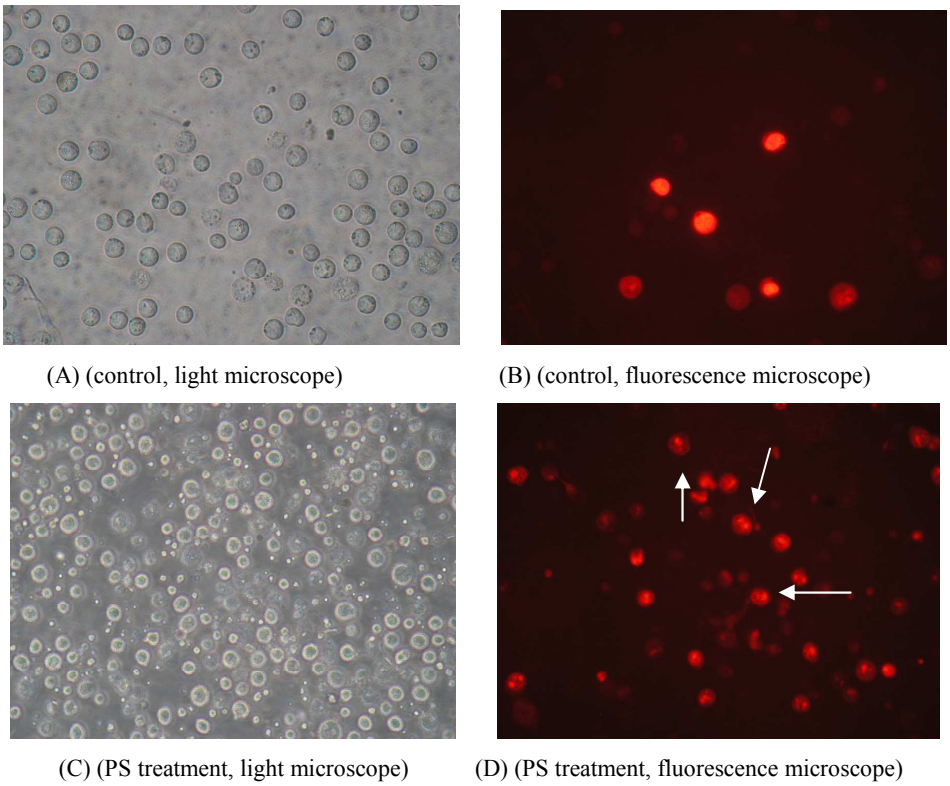

Fig.3 Morphological variation of K562 cells with PI staining. PI Staining of K562 cells were treated with PS for 24h with concentration of 100 μg/ml. Untreated cells were used as control. Cell morphology was determined by microscopy. (A) control (×20 objective lens) with light microscope observation. (B) Control (×20 objective lens) with fluorescence microscope. (C) Cells treated with PS for 24h (×20 objective lens) with light microscope observation. (D) Cells treated with PS for 24h (×20 objective lens) with fluorescence microscope.

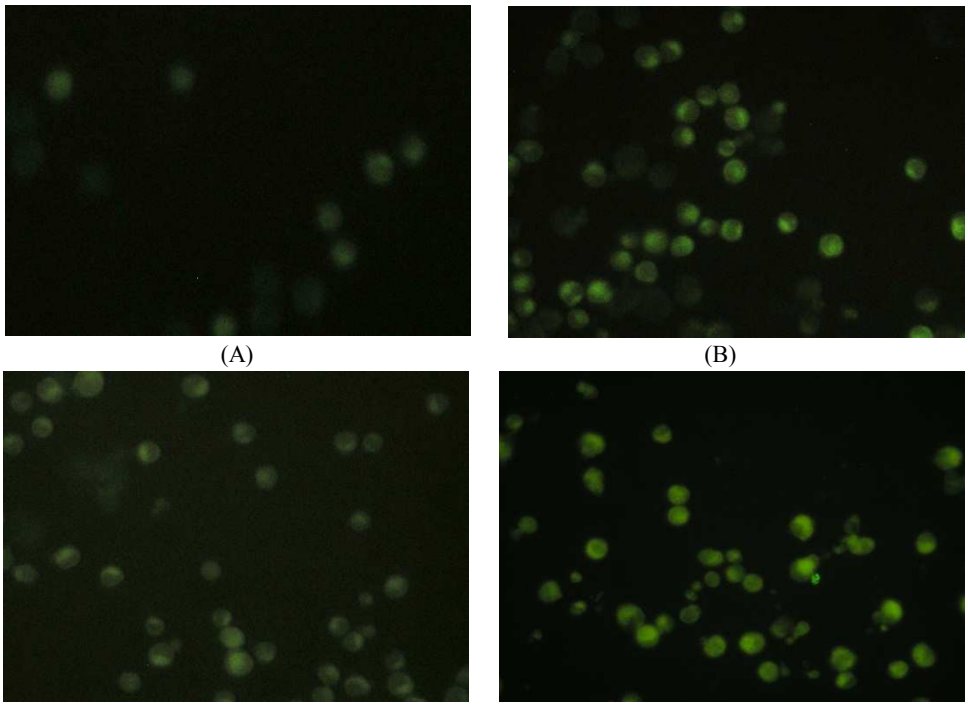

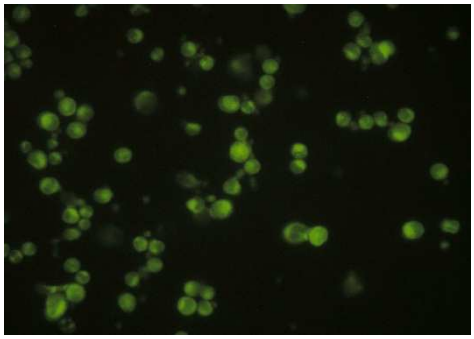

(E)

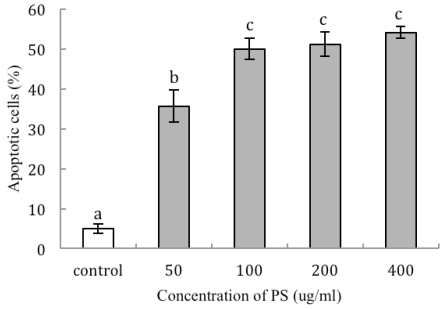

(F)

Fig.4 Effect of K562 cells apoptosis induced by low dose cartilage polysaccharide by TUNEL staining. TUNEL staining of K562 cells with or without PS. K562 cells were cultured for 24 h with PS: 50 μg/ml (B), 100 μg/ml (C), 200μg/ml (D) or 400 μg/ml (E), untreated cells were used as control (A). After treatment, K562 cells were isolated and prepared for measurement of TUNEL staining using fluorescence microscopy (magnification, ×40). Apoptotic rate was calculated as apoptotic cell number /total cell number (F) (mean ±SD, n = 3). Bars with no letters in common are significantly different ($p < 0.05$).

3.5 Effect of PS on oxidative metabolism balance

To determine the relationship between PS-induced K562 cell apoptosis and oxidative metabolism, superoxide anions, SOD and CAT prepared from the cells exposed to PS for various times were detected. It is well-recognized that superoxide anions are produced by biochemical reactions in the mitochondria and are converted to other type of ROS by antioxidase. As indicated in Fig. 5, the superoxide anion concentrations of control group displayed minor changes, whereas these levels increased in the PS-treated groups in a treatment time-dependent manner. There was a significant difference in the superoxide anion concentrations between the control and PS-treated cells at 12 h. The PS-treated cells maintained higher levels with significant increases from 24 to 48 h after the treatment. The SOD concentrations were significantly different between the control and PS-treated groups at each of the time intervals. After treatment with PS, SOD activity increased rapidly to 50±5.69 mol/10^6 cells at 12 h and then significantly decreased to 42.33±1.38 mol/10^6 cells and 10.17±1.41 mol/10^6 cells at 24 h and 48 h, respectively (Fig. 6). The CAT concentrations of the PS-treated cells were significantly higher than those of the control cells from 12 to 24 h (Fig. 7). After 48 h, the CAT concentrations of the experimental group decreased to 6.50± 0.12, which was similar to the initial level. The CAT level of the control group increased gradually across the entire experimental, whereas the CAT levels of the experimental group were increased at 24 h and then decreased at 48 h.

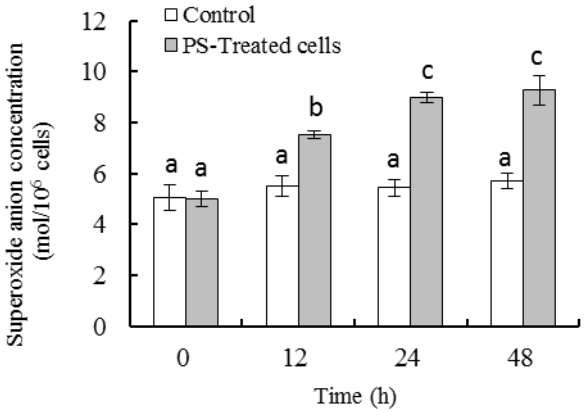

Fig.5 Effect of PS on superoxide anion concentration of K562 cells. K562 cells were treated with 12.5μmol/l Cytochrome C and 100μg/ml of PS for 12h, 24h and 48h. Plates were read at 550nm and no PS wells were used as control. (mean ± SD, n = 3). Bars with no letters in common are significantly different ($p < 0.05$).

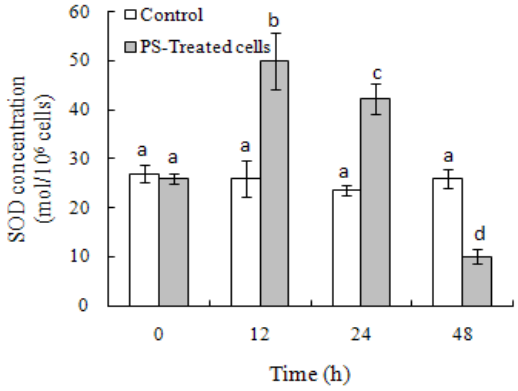

Fig.6 Effect of PS on SOD concentration of K562 cells. Cells were incubated with 100μg /l PS for 12h, 24h and 48h and lysed by Triton X-100. The supernatant was obtained after centrifugation, and SOD concentration was measured according to the instruction of the kit. (mean ± SD, n = 3). Bars with no letters in common are significantly different ($p < 0.05$).

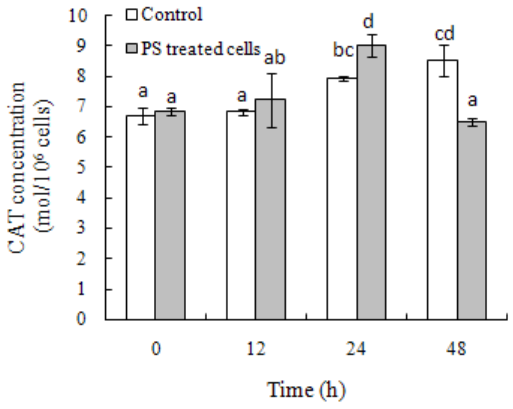

Fig.7 Effect of PS on CAT concentration of K562 cells. Cells were incubated with 100μg /l PS for 12h, 24h and 48h and lysed by Triton X-100. The supernatant was obtained after centrifugation, and CAT activity was detected according to H_2O_2 consumption by using a automated spectrophotometer plate reader. (mean ± SD, n = 3). Bars with no letters in common are significantly different ($p < 0.05$).

3.6 Roles of caspases in PS-induced apoptosis

It has been shown that caspases-3 and -7, which are both effector caspases, are cleaved by the initiator caspases-8 and -9 into active forms. Although caspases-3 and -7 play different roles in the execution of apoptosis, they have similar substrate specificities and structures. Thus, in the present study, the caspase-Glo-3/7 kit with z-DEVD-R110 was used to assay the caspase-3/7 activity to determine the extent of apoptosis. As shown in Fig. 8A, after treatment with the PS, the caspase-3/7 activity initially increased and then ultimately decreased. There was no significant difference between the control (1.01 ± 0.11) and experimental groups after 12 h of treatment (1.11 ± 0.12), but caspase-3/7 increased remarkably after 24 h of incubation with the PS (3.99 ± 0.14), indicating that apoptosis occurred in these K562 cells. This finding is in accordance with the results of PI staining, which revealed typical apoptotic morphologies in the mass cancer cells following 24 h of treatment (Fig. 3D). After reaching the peak value, the caspase-3/7 activity decreased rapidly to 1.39 ± 0.09, which may be due to fact that the K562 cells possessed reduced enzymatic activity at the end-stage of apoptosis. Combing with those illustrated in Fig. 3D and Fig. 4, these results clearly demonstrate the apoptotic morphologies and severe nuclear shrinkage of end-stage apoptosis. The occurrence of apoptosis was further suggested that PS-induced K562 cell apoptosis inhibited the proliferation of these cells. There are two major apoptosis signaling pathways; i.e., the mitochondrial pathway and the death receptor pathway. Caspase-9 is located at the top of caspase cascade, is a key protease in the mitochondrial apoptosis pathway, and the activation of caspase-9 is particularly important for the downstream pathway. In addition, as part of the death–inducing signaling complex, caspase-8 can be spontaneously activated followed by the downstream caspase-3, which ultimately acts upon the PARP substrate or other substrates in the cell nucleus, thereby causing them to split and inducing apoptosis. Because caspase-3 was detected, we investigated the involvement of caspase-9 and caspase-8 in PS-induced apoptosis. As shown in Fig. 8B, the activations of caspase-9 and caspase-8 were determined via measurements of the active forms of caspase-9 and caspase-8, respectively, with a luminescent assay kit. Both of these caspases were significantly activated after 24 h, and these findings are in accordance with the results shown in Fig. 3 D demonstrating the typical apoptotic morphology and the detection of the 3'-OH end via TUNEL labeling shown in Fig. 4.

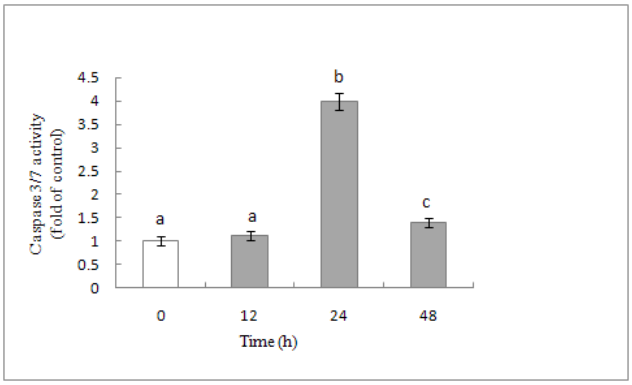

(A)

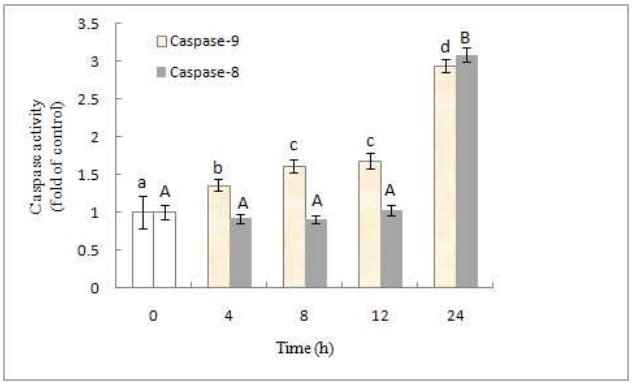

(B)

Fig.8. PS induces apoptosis by trigering the activation of caspase-3/7, 8 and caspase-9. After preincubation with or without 100μg/ml PS for 4, 8, 12, 24, or 48 h, the K562 cells were centrifuged and 100 μl of caspase-Glo 3/7, 8, 9 reagent was added to the precipitate of each well. The context of the wells were mixed well and were then incubated at room temperature for 1 h. Plate-reading luminometer was used to detect activities of caspase-3/7, caspase-8 and caspase-9. Multiples of enzyme activity increased = (assay value – blank value) / (negative control value – blank value). (mean ± SD, n = 3). Bars with no letters in common are significantly different ($p < 0.05$).

3.7 Discussion

In the present study, we investigated the involvement of the redox system in the mitochondria-mediated caspase pathway. HPLC was used to quantify the components of the PS extract from porcine cartilage. The PS was composed of 95% chondrotin sulfate. The MTT results demonstrated that the PS had a noticeable effect on the growth inhibition rate of K562 cells at the lower concentration of 50 μg/ml. Morphological and biochemical changes indicated the presence of apoptosis, such as membrane blebbing, cell shrinkage and the presence of 3'-OH terminals, were been observed and confirmed with PI staining and TUNEL assays, respectively, in the PS-treated K562 cells. Cell survival depending on the balance between the ROS that are generated internally and antioxidative

metabolism, and this balance is reflected by the redox state level.[33] Tumor cell might excrete some amounts of ROS, such as O^{2-} and H_2O_2, through autocrine mechanisms in addition to the ROS that are secreted following stimulation. Cancer cells, particularly those with the features of high invasibility and high transitivity, might generate large but endurable amounts of ROS. As signal molecules, ROS can activate other sensitive transport factors[34] or genes that cause cells to proliferate, die or undergo apoptosis. [35] Lower concentrations of ROS stimulate cell proliferation. Some studies have reported that high levels of hydrogen peroxide inhibit the proliferation of cancer cells, but these finding remain controversial because other results have demonstrated that cancer cell growth can be suppressed by the clearance of H_2O_2.[36,37] Because SOD can eliminate O^{2-} by converting it to H_2O_2 and also PS induced the K562 cells to produce abundant O^{2-}, we conclude that PS inhibited K562 proliferation by inducing the autocrine release of large amounts of superoxide anions. After incubation with PS, the K562 cells produced massive amounts of superoxide anions, and to eliminate this ROS. The cells were then stimulated to generate certain amounts of the antioxidases SOD and CAT. With the increase in the superoxide anion level, the intracellular balance between ROS and antioxidases was severely disrupted, which led to rapid decreases in SOD and CAT activities. Cancer cell cannot endure strong oxidative stresses; thus, the nuclear DNA, RNA and protein were irreversibly destroyed, and plus, the ROS also stimulated the cells directly and functioned together as apoptotic signals that changed the permeability of the mitochondrial outer membranes, which released apoptotic factors into the cytoplasm and induced apoptosis. [38] In this study, we first reported caspase-3/7 expression and the presence of caspase-dependent apoptosis (Fig. 8A) along with both caspase 8 and 9 detected, illustrating that both intrinsic and extrinsic pathways were involved in the PS-induced apoptosis.

Conclusions

In summary, PS was successfully isolated from porcine cartilage, and the yield and purity were detected. The in vitro antitumor mechanisms and related oxidative metabolic effects of the PS were elaborated. The present study demonstrated that PS-induced K562 apoptosis achieved from the activation of the ROS-mediated caspase mitochondrial pathway. These results provide new insight into the possible molecular mechanisms and signaling pathways of PS-induced apoptosis.

Acknowledgements

This work was supported by grant from the National Natural Science Foundation of China (No. 20576101), the Special Financial Grant from the China Postdoctoral Science Foundation (2013T60383), the Fundamental Research Funds for the Central Universities (Grant No. HIT. NSRIF. 2013107) and the China Postdoctoral Science Foundation under General Financial Grant (Number 2012M510976).

Notes and references

[a] School of Food Science and Engineering, Harbin Institute of Technology, Harbin 150090, China. E-mail: weisong@hit.edu.cn; Tel: +86-451-86282908

[b] Key Laboratory of Food Nutrition and Safety, Ministry of Education, Tianjin University of Science and Technology, Tianjin 300457, China. E-mail: anjun_liu@yahoo.com; Tel: +86-22-60272191

[c] Department of Biosystems Engineering and Soil Science, University of Tennessee, 2506 E.J.Chapman Drive, Knoxville, TN 37996,USA

1. P. Shao, X. Chen and P. Sun, *Carbohydrate Polymers*, 2014, 105, 260-269.
2. T. Zhao, G. Mao, R. Mao, Y. Zou, D. Zheng, W. Feng, Y. Ren, W. Wang, W. Zheng, J. Song, Y. Chen, L. Yang and X. Wu, *Food and Chemical Toxicology*, 2013, 55, 609-616.
3. D. Wang, S.-Q. Sun, W.-Z. Wu, S.-L. Yang and J.-M. Tan, *Carbohydrate Polymers*, 2014, 105, 127-134.
4. A. Patel, J. B. Prajapati, O. Holst and A. Ljungh, *Food Bioscience*, 2014, 5, 27-33.
5. T. Hardingham and A. Fosang, *The FASEB Journal*, 1992, 6, 861-870.
6. R. A. A. Muzzarelli, F. Greco, A. Busilacchi, V. Sollazzo and A. Gigante, *Carbohydrate Polymers*, 2012, 89, 723-739.
7. A. Zhang, N. Xiao, P. He and P. Sun, *International Journal of Biological Macromolecules*, 2011, 49, 1092-1095.
8. J. Zhang, Y.-j. Liu, H.-s. Park, Y.-m. Xia and G.-s. Kim, *Carbohydrate Polymers*, 2012, 87, 1539-1544.
9. H. Zhang, Z.-Y. Wang, Z. Zhang and X. Wang, *Carbohydrate Polymers*, 2011, 84, 638-648.
10. W. Song, Y. Jia, Y. Fan, M. Du and A. Liu, *Journal of Functional Foods*, 2013, 5, 1270-1278.
11. A.-J. Liu, W. Song, N. Yang, Y.-J. Liu and G.-R. Zhang, *Cell biology and toxicology*, 2007, 23, 465-476.
12. Y. Zhao, X. Sui and H. Ren, *Journal of cellular physiology*, 2010, 225, 316-320.
13. I. R. Indran, G. Tufo, S. Pervaiz and C. Brenner, *Biochimica et Biophysica Acta (BBA) - Bioenergetics*, 2011, 1807, 735-745.
14. M. E. Delgado, M. Olsson, F. A. Lincoln, B. Zhivotovsky and M. Rehm, *Biochimica et Biophysica Acta (BBA) - Molecular Cell Research*, 2013, 1833, 2279-2292.
15. C.-J. Hsieh, P.-L. Kuo, Y.-C. Hsu, Y.-F. Huang, E.-M. Tsai and Y.-L. Hsu, *Free Radical Biology and Medicine*, 2014, 67, 159-170.
16. L. Yuan, J. Wang, H. Xiao, W. Wu, Y. Wang and X. Liu, *Food and Chemical Toxicology*, 2013, 53, 62-68.
17. L. Liu, J. Fu, T. Li, R. Cui, J. Ling, X. Yu, H. Ji and Y. Zhang, *European Journal of Pharmacology*, 2012, 691, 61-68.
18. N. Hempel and J. A. Melendez, *Redox Biology*, 2014, 2, 245-250.
19. M. L. Circu and T. Y. Aw, *Seminars in Cell & Developmental Biology*, 2012, 23, 729-737.
20. T. R. Figueira, M. H. Barros, A. A. Camargo, R. F. Castilho, J. C. Ferreira, A. J. Kowaltowski, F. E. Sluse, N. C. Souza-Pinto and A. E. Vercesi, *Antioxidants & redox signaling*, 2013, 18, 2029-2074.
21. T. Yamada, N. Egashira, M. Imuta, T. Yano, Y. Yamauchi, H. Watanabe and R. Oishi, *Free Radical Biology and Medicine*, 2010, 48, 120-127.
22. N. Bogurcu, C. Sevimli-Gur, B. Ozmen, E. Bedir and K. S. Korkmaz, *Biochemical and Biophysical Research Communications*, 2011, 409, 738-744.
23. K. Perumal Vijayaraman, S. Murugananthan, M. Subramanian, K. P. Shunmugiah and P. D. Kasi, *Ecotoxicology and Environmental Safety*, 2012, 86, 79-85.
24. P.-L. Kuo, C.-Y. Chen and Y.-L. Hsu, *Cancer research*, 2007, 67, 7406-7420.
25. B. M. Kim, Y. J. Choi, Y. Han, Y.-S. Yun and S. H. Hong, *Toxicology and Applied Pharmacology*, 2009, 239, 87-97.
26. Y.-F. Wang, H.-W. Shyu, Y.-C. Chang, W.-C. Tseng, Y.-L. Huang, K.-H. Lin, M.-C. Chou, H.-L. Liu and C.-Y. Chen, *Toxicology and Applied Pharmacology*, 2012, 259, 177-186.
27. N. Yadav and D. Chandra, *Mitochondrion*, 2014, 16, 18-25.
28. K.-J. Won, K.-S. Chung, Y. S. Lee, M. S. Alia, M. K. Pervez, S. Fatima, J.-H. Choi and K.-T. Lee, *Chemico-Biological Interactions*, 2010, 188, 505-511.
29. Y. J. Kang, I. Y. Kim, E. H. Kim, M. J. Yoon, S. U. Kim, T. K. Kwon and K. S. Choi, *Experimental & molecular medicine*, 2011, 43, 24-34.

30. D.-M. Zhu, J. Shi, S. Liu, Y. Liu and D. Zheng, *PloS one*, 2011, 6, e18291.
31. W. Pang, X. Leng, H. Lu, H. Yang, N. Song, L. Tan, Y. Jiang and C. Guo, *Neuroscience Letters*, 2013, 552, 140-145.
32. S. Szücs, C. Varga, I. Ember and P. Kertai, *Journal of immunological methods*, 1994, 167, 245-251.
33. K. Niforou, C. Cheimonidou and I. P. Trougakos, *Redox Biology*, 2014, 2, 323-332.
34. D.-Y. Lu, C.-S. Chang, W.-L. Yeh, C.-H. Tang, C.-W. Cheung, Y.-M. Leung, J.-F. Liu and K.-L. Wong, *Phytomedicine*, 2012, 19, 1093-1100.
35. A. Iwamaru, E. Iwado, S. Kondo, R. A. Newman, B. Vera, A. D. Rodríguez and Y. Kondo, *Molecular cancer therapeutics*, 2007, 6, 184-192.
36. W. C. Burhans and N. H. Heintz, *Free Radical Biology and Medicine*, 2009, 47, 1282-1293.
37. M. Kamiński, M. Kießling, D. Süss, P. H. Krammer and K. Gülow, *Molecular and cellular biology*, 2007, 27, 3625-3639.

